Accepted for publication in *Canadian Mineralogist*, scheduled for February 2007.
See *Canadian Mineralogist* **45**(2) 379-389 (2007) for final version.

# MICRO- AND NANO-SCALE GRAPHITE CONES AND TUBES FROM HACKMAN VALLEY, KOLA PENINSULA, RUSSIA

John A. JASZCZAK[§]
*Department of Physics and the A. E. Seaman Mineral Museum, Michigan Technological University, Houghton, Michigan, 49931-1295, USA*

Svetlana DIMOVSKI[†]
*Department of Materials Science and Engineering and A.J. Drexel Nanotechnology Institute, Drexel University, 3141 Chestnut St., Philadelphia, Pennsylvania 19104, USA*

Stephen A. HACKNEY
*Department of Materials Science and Engineering, Michigan Technological University, Houghton, Michigan, 49931-1295, USA*

George W. ROBINSON
*Department of Geological and Mining Engineering and Sciences, and the A. E. Seaman Mineral Museum, Michigan Technological University, Houghton, Michigan, 49931-1295, USA*

Paolo BOSIO
*Via G. Mameli 52, 21010 Cardano al Campo (VA), Italy*

Yury GOGOTSI
*Department of Materials Science and Engineering and A.J. Drexel Nanotechnology Institute, Drexel University, 3141 Chestnut St., Philadelphia, Pennsylvania 19104, USA*

[§]*E-mail address:* jaszczak@mtu.edu
[†]*Present address*: The Procter and Gamble Company, Corporate Analytical, 11810 E. Miami River Rd., Mailbox 192, Cincinnati, Ohio 45252

## ABSTRACT

Several unusual forms of natural graphite from an alkaline pegmatite that crosscuts rischorrite in the Hackman Valley, Khibiny Massif, Kola Peninsula, Russia are described. The graphite occurs macroscopically in two forms: as spherical aggregates up to 2 cm in diameter of friable, radially-aligned fibers ~20 μm in cross section, and as fine-grained surface coatings in cavities covering aegirine, strontian fluorapatite and K-feldspar. Optical microscopy and field emission scanning electron microscopy (FESEM) show that the fibers are actually hollow channels whose walls are composed of tabular graphite crystals greatly elongated in the direction of the fiber axis and with their basal planes oriented parallel to the channel walls. Inside and among the channels occur rolled graphitic structures (RGS): scrolls, tubes, and cones, up to 2 μm in diameter and up to 15 μm in length. The fine-grained graphite coatings on the surfaces of cavities, on the other hand, consist almost solely of micro- and nano-scale RGS. The largest of the RGS are hollow scrolls, with the c-axis predominantly perpendicular to the scroll axis. These are usually cigar shaped but can also be more tubular. Conical RGS occur at the micro- and nano-scales. The nano-scale cones tend not to be hollow and may have a cone-helix structure. Transmission electron microscopy (TEM), Raman spectroscopy, and FESEM indicate that the RGS are composed of well-ordered graphitic layers but are commonly coated by amorphous carbon. The morphologies and paragenesis of these unusual graphite forms suggest a possible hydrothermal origin.

*Keywords*: graphite, electron microscopy, crystal growth, crystal morphology, Raman spectroscopy, stable carbon isotopes

## INTRODUCTION

Synthetically grown graphite and graphitic materials constitute an ever expanding family of microstructures and morphologies ranging from nano-scale tubes (Dresselhaus *et al.* 2001, Harris 1999, Iijima 1991, Oberlin *et al.* 1976), onions (Ugarte 1995), cones (Krishnan *et al.* 1997), conical fibers (Endo *et al.* 2002, Zhang *et al.* 2003) and horns (Iijima *et al.* 1999) to larger scale whiskers (Bacon 1960, Speck *et al.* 1989), cones (Gillot *et al.* 1968), spheres (Möschel *et al.* 2001, Jaszczak 1995), and other unusual structures (Gogotsi *et al.* 2000). The materials and references cited above are by no means exhaustive. Reports of unusual naturally occurring graphite have been growing in number as well. These include barrel-shaped crystals (Palache 1941, Jaszczak 2001), skeletal overgrowths on tabular crystals (Weis 1980, Jaszczak 1997), spheres (Kvasnitsa *et al.* 1998, Jaszczak 1995), triskelia (Jaszczak & Robinson 2000), whiskers (Patel & Deshapande 1970), and cones (Jaszczak *et al.* 2003). This

paper reports the discovery of several additional morphologies for natural graphite: hollow channel-like fibers and micro- and nano-scale structures composed of stacked but intrinsically curved graphene (a single layer of $sp^2$-bonded carbon atoms, which when stacked in an ABAB sequence forms graphite) sheets. The latter form scrolls, tubes, and cones. As there is no standardization of nomenclature for the ever increasing variety of exotic graphitic structures, we shall collectively refer to the graphitic scrolls, tubes, and cones as "rolled graphitic structures" (RGS).

## GEOLOGY

The samples described herein were obtained from a graphite-bearing alkaline pegmatite near the bed of Hackman Creek in the Hackman Valley on the eastern slope of Mt. Yukspor, Khibiny Massif, Kola Peninsula, Murmansk, Russia (Kostyleva-Labuntsova *et al.* 1978, Yakovenchuk *et al.* 1999, Yakovenchuk *et al.* 2005). Covering an area of 1,327 $km^2$, the Khibiny pluton is the Earth's largest alkaline intrusion and comprises two mountain ridges that are arcuate in plan, and open towards the east. This alkaline complex is a concentrically zoned multiphase Devonian intrusion, derived from a huge body of silica-undersaturated magma, emplaced in Archean granitic gneisses at the contact with Proterozoic volcanic-sedimentary complexes (Kramm & Kogarko 1994, Kogarko *et al*. 1981). The arcuate alkalic intrusives comprise a complex of coarse-grained nepheline syenites (i.e., khibinites, trachytic khibinites, foyaites, and lyavchorrites, and rischorrites) associated with ijolite-urtite-melteigites and apatite-nepheline rocks of enigmatic origin, carbonatites, a hornfelsic outer contact, and fenite (Yakovenchuk *et al.* 2005, Galakhov 1975, Zak *et al*. 1972).

Pegmatites are widespread at Khibiny, and they are particularly abundant in foyaites and rischorrite zones. The graphite-bearing pegmatite of interest to the present study consists of a 10-50 cm-wide aegirine-feldspar pegmatite vein that crosscuts rischorrite (Yakovenchuk *et al.* 2005). Associated minerals include aegirine, strontian fluorapatite, natrolite, K-feldspar, and minor amounts of mica and other minerals. Graphite with a similar macroscopic appearance occurs in aegirine-rich sections of albite veins at the Kola Peninsula's Mt. Takhtarvumchorr (see photograph in Yakovenchuk 2005, p. 80), but we have not had the opportunity to examine actual samples.

## EXPERIMENTAL METHODS

After mechanical trimming, samples were examined by field emission scanning electron microscopy (FESEM) (FEI XL-30, FEI-Sirion 200, JEOL JSM-7000F, and Hitachi S-4700). During mechanical trimming of samples, a characteristic "rotten egg" odor of $H_2S$ could be detected. Most samples were lightly gold coated before FESEM examination. RGS-rich graphite scraped from cavities in the host rock resulted in a powder that was directly placed on lacy carbon-coated copper grids for examination by transmission electron microscopy (TEM) (JEOL JSM-4000FX at 200.0 kV). Raman spectroscopy was employed to characterize the graphite using a Renishaw 1000 microspectrometer, with an $Ar^+$ laser 514.5 nm excitation wavelength and 2-μm spot size. Polarized light microscopy (Nikon Optiphot-Pol) was used to examine channel-like fibrous graphite in polished sections of the host rock. Crushed and powdered samples of the channel-like fibrous graphite were submitted to Geochron Laboratories (Cambridge, MA) for bulk stable carbon isotope analyses.

## RESULTS AND DISCUSSION

The graphite at Hackman Valley occurs in two macroscopic forms. The first is as spherical aggregates ranging in diameter from 3 mm to 2 cm, and composed of friable, radially-aligned fibers (Fig. 1a). FESEM shows that these fibers are actually hollow channels composed of tabular graphite crystals greatly elongated in the direction of the fiber axis and with their basal planes oriented parallel to the channel walls (Fig. 1b-d). Reflectance dichroism of the graphite channels in polished cross section also indicates that the basal planes are parallel to the channel walls. The fibers range in size from 10 to 60 μm across, and have cross-sectional shapes that are polyhedral, misshapen or crushed (Fig. 1b,c). The graphite fibers tend to be brittle, and some appear to be naturally broken (Fig. 1b). The brittleness is attributed to a secondary fine-grained overgrowth of graphite on the surfaces of the tabular graphite crystals (Fig. 1d). Inside and among the hollow channels occur numerous RGS up to 4 μm in length and up to 1.5 μm in diameter (Fig. 1b,c) in clusters or in isolation, and protruding from the secondary-graphite overgrowth (Fig. 1e). Although the channels are typically empty, some are filled with aegirine or strontian fluorapatite (Fig. 1f). This graphite type may be an overgrowth or replacement of earlier-grown crystals, such as aegirine, apatite or lamprophyllite, all of which occur as radially-aligned aggregates of prismatic crystals at several occurrences in the Kola Peninsula (Kostyleva-Labuntsova *et al.* 1978, Yakovenchuk *et al*. 1999, Yakovenchuk *et al.* 2005). Individual aegirine crystals partly overgrown with graphite are also common in the graphitic host rock (Fig. 2). The second macroscopic form of graphite is what appears optically as fine-grained surface coatings in aegirine-rich cavities associated with apatite, feldspar, annite, and white whisker crystals of an unidentified sodium-titanium-aluminum-silicate (possibly vinogradovite). However, FESEM reveals that these graphitic coatings almost solely consist of micro- and nano-scale RGS (Fig. 3a). The RGS' morphologies range from conical to cigar-like, to tubular,

and their sizes range from tens of nanometers in length and diameter to over 10 μm in length and several μm in diameter. Their tips are typically rounded (Fig. 3b), but can be relatively sharp as well (Figs. 3d-g). Many RGS also show a change in morphology at their tips (Fig. 3d-h).

A relatively large broken tube almost 2 μm long and ~0.5 μm in diameter is visible at the center right of Figure 3a. Hollowness is also evident from the depressions formed where RGS have broken off from the secondary graphite overgrowths on the hollow-channel fibers (Fig. 1e). Fractured tubular or cigar-shaped RGS show that the graphene sheets are aligned predominantly circumferentially around the tube axis (Fig. 3c), and suggest a scroll type structure as described by Bacon (1960) for laboratory-grown graphite whiskers in a d.c. arc. Some RGS show a distinct spiral-contour at the tips that is also suggestive of a scroll-type structure [Fig. 3h; compare Haanstra *et al.* (1972) Fig. 13]. Both scroll-type and cone-helix structures provide attractive models for their growth since the edges of graphene sheets are continuously exposed at the side surfaces and at the tips to provide favorable growth sites for thickening and lengthening of the RGS.

TEM indicates that the graphite in the nano-scale cones is well-ordered. Figure 4a shows a TEM image of a ~200-nm diameter cone with a 60° apex angle. The corresponding selected area electron diffraction pattern from the center of this cone is shown in Figure 4b. Strong (00*l*) and (10*l*) diffraction spots indicate that the cone is graphitic and well-ordered. The two sets of (*00l*) diffraction spots come from graphene sheets of the cone walls that are locally parallel to the electron beam. The angle between the lines that connect these two sets of spots corresponds to the relative inclination of the graphene sheets in the cone walls, and is the same as the cone's apex angle. This implies that the graphene sheets are indeed parallel to the conical surfaces. High resolution TEM (HRTEM) lattice fringes likewise indicate that the graphene sheets are arranged parallel to the conical surfaces in the nanocones (Fig. 4c,d). Significant disorder is evident in the central cone axis regions (Fig. 4d) and at the surfaces, which in some cones appear to be coated with several nanometers or more of amorphous carbon. The average (002) interplanar spacing ($d_{002}$) measured from lattice fringes of a 39° nanocone (Fig. 4c) is 3.56 ± 0.12 Å, and that from less-ordered lattice fringes of a 126° nanocone (Fig. 4d) is 3.79 ± 0.14 Å. These values are significantly larger than ideal graphite's $d_{002}$ of 3.35 Å. Possible reasons for this include the moderate to high degree of disorder present, and the likely non-ideal stacking of the graphene sheets, as discussed below.

A cone-helix model (Fig. 5) has been proposed to describe the structure of laboratory grown (Double & Hellawell 1974) and naturally occurring (Jaszczak *et al.* 2003) graphite cones. In this model, a graphene sheet is wound around an axis in a helical structure, similar to one that would be formed by a [001] screw dislocation in graphite. However, unlike the case of simple screw dislocation, adjacent graphene layers are rotated with respect to each other by an overlap angle θ, which is geometrically related to the cone's apex angle α by $\alpha = 2\sin^{-1}(1-\theta/360°)$. Certain values of $\theta = n\times60° \pm \omega$, where n = 0, 1, ... 6, and ω = 0°, 13.2°, 21.8° or 27.8°, result in a high density of lattice coincidences between layers and are thus expected to have relatively low-energies making certain apex angles more favorable than others (Double & Hellawell 1974, Jaszczak *et al.* 2003, Ekşioğlu & Nadarajah 2006). The apex angles of some of the nanocones from Hackman Valley that were measurable (ca. 39°, 60°, and 126°; Fig. 3) are consistent with this model. It is also possible that the micron-sized RGS are actually cone-helix structures with very large θ values. (Note that θ = 360° would correspond to a scroll or tube structure with α = 0°.) However, while fractured, large-apex-angle cone-helix structures typically break in such a fashion as to reveal cone-shaped fracture surfaces (Dong *et al.* 2002, Haanstra *et al.* 1972, Gillot 1968), conical fracture surfaces are not evident in broken, micron-sized RGS from Hackman Valley (Fig. 2c). The cone-helix structures generally do not have an ABAB stacking of graphene sheets unless θ=n×60°. These fundamental structural aspects are expected to lead to larger-than-ideal interplanar spacings as is common in twist grain boundaries in many materials (Wolf 1984, Wolf 1989, Wolf 1990, Phillpot *et al.* 1990, Astala & Bristowe 2002); however, we are unaware of any systematic investigations of (001) twist grain-boundary energies and d-spacings in graphite *per se*. In turbostratic graphite, which is composed of planar graphene sheets rotated randomly with respect to each other, the average $d_{002}$ is approximately 3.44 Å (Franklin 1951). Likewise, the 002 interplanar spacing for graphene sheets in nested carbon nanotubes (Saito *et al.* 1993), benzene-derived carbon fibers (Speck *et al.* 1989), and synthetic graphite cones (Terrones *et al.* 2001) can approach or exceed that of turbostratic graphite. Well-ordered catalytically-grown graphite fibers, whose c-axes are parallel to the fiber axes, were recently reported to also have a relatively large average $d_{002}$ value of 3.42 ± 0.09 Å (Anderson 2006). The cause of the even larger $d_{002}$ values for the nanocones of this study is the subject of continuing investigation, as is the $d_{002}$ value for the micron-sized RGS, which is difficult to measure and is currently unknown.

The first- and second-order Raman spectra from a micron-sized Hackman Valley rolled graphitic structure are given in Figure 6. For reference, also given is the Raman spectrum from a graphite cone from Gooderham, Ontario and the basal plane of a single crystal of graphite. The spectra of the Hackmen Valley RGS are similar to those from microcrystalline graphite, and show little variation with respect to apex angle (Jaszczak *et al.* 2003). Peak positions and peak widths were consistently reproducible over many spectra from different RGS in the samples. Almost all of the observed Raman modes can be assigned according to the selection rules and the double resonance Raman mechanism (Tan *et al.* 2004, Thomsen & Reich 2000, Nemanich & Solin 1979). The first-order region of the spectra from the RGS shows a strong, narrow, slightly upward shifted (relative to single crystals)

graphitic (G) ~1583 $cm^{-1}$ line, as well as a prominent disorder-induced peak (D) at ~1360 $cm^{-1}$. Full width at half maximum (FWHM) of the G line was measured to be ~33 $cm^{-1}$ for cones and ~24 $cm^{-1}$ for scroll-type RGS, as compared to 14 $cm^{-1}$ for a graphite single crystal. The calculated value of the D/G line intensity ratio ($R$) is slightly higher for Gooderham cones ($R$ = 0.30) than for Hackman Valley RGS ($R$ = 0.25) indicating somewhat higher degree of graphitic order in the latter.

Stable carbon isotope analyses of four crushed and powdered fibrous graphite samples were performed at Geochron Laboratories and yielded an average $\delta^{13}C = -15.1 \pm 0.6‰$ PDB. Chukhrov *et al.* (1984) reported a somewhat lower value of −18.0‰ for graphite from the Kola Peninsula's "Gakman Valley", and values of −11.9 and −18.5‰ for graphite from Mt. Takhtarvumchorr. These values are intermediate between the two biogenic reservoirs of crustal carbon: reduced organic carbon and carbonate-derived carbon, and are consistent with C-O-H fluid-deposited graphite deposits in metasedimentary and plutonic rocks such as those in central New Hampshire (Rumble *et al.* 1986, Rumble & Hoering 1986, Duke & Rumble 1986).

## SUMMARY AND CONCLUSIONS

Graphite from an alkaline pegmatite in the Hackman Valley, Khibiny Massif, Kola Peninsula, Russia occurs in two unusual forms. The first is as fiber-like hollow channels up to 20 μm in cross section in radially-aligned spherical aggregates that occur up to 2 cm in diameter. The walls of the channels are composed of tabular graphite crystals greatly elongated in the direction of the fiber axis, and typically also show a fine-grained secondary overgrowth. This type of graphite may be a pseudomorphic overgrowth or replacement of earlier-grown crystals, particularly aegirine or fluorapatite. The second form of graphite is as scrolls, tubes and cones, which we have generically referred to as rolled graphitic structures (RGS). The Hackman Valley RGS, which range in size from 100 nm to 2 μm in diameter, and from 200 nm to 15 μm in length, occur in and on the hollow graphite channels, and also as fine-grained coatings on aegirine crystals in small 1 to 3 mm cavities in the host rock. The morphologies of the graphite, the petrological associations, and the $\delta^{13}C$ values suggest that the graphite channels and RGS in the pegmatite were deposited from a hydrothermal C-O-H fluid by any of a variety of mechanisms, which could include cooling, hydration reactions with the country rock, or mixing of C-O-H fluids from different sources (Luque *et al.* 1998). In contrast to this relatively small deposit of graphite in the Hackman Valley, large scale fluid-deposited epigenetic graphite deposits are typically of very high crystallinity (Luque *et al.* 1998, Pasteris 1999). Hydrothermal growth of both planar graphite and RGS has been demonstrated in laboratory conditions (Libera & Gogotsi 2001) using Ni powder as a catalyst. Ni, Fe, and Co are commonly used catalysts for the growth of carbon nanotubes (Dresselhaus *et al.* 2001, Harris 1999) and conical RGS in other synthesis routes as well (Zhang *et al.* 2003, Endo *et al.* 2002). We were unable to detect any transition metal elements in the Hackman Valley RGS using energy dispersive x-ray spectroscopy on either the FESEM (operating at 20 kV) or on the TEM, although Fe is present in associated minerals like aegirine and annite. The nucleation mechanism of and detailed growth conditions for these exotic natural structures remain to be further investigated.

## ACKNOWLEDGMENTS

We are grateful to Dmitriy Belakovskiy, Mathias Rheinlander, Steffen Möckel, Roland Dietrich, and Dmitriy Lisitsin for providing samples. We thank editor Robert Martin and referees Victor Yakovenchuk and Kimberly Tait for their thoughtful reviews that improved this manuscript. Work done at Michigan Tech was supported in part by the Edith Dunn and E. Wm. Heinrich Mineralogical Research Trust and the Michigan Tech Applied Chemical and Morphological Analysis Laboratory. Work done at Drexel was supported by the U.S. Department of Energy.

## REFERENCES

ANDERSON, P.E. (2006): A method for characterization and quantification of platelet graphite nanofiber edge crystal structure. *Carbon* **44**, 2184-2190.

ASTALA, R. & BRISTOW, P.D. (2002): A computational study of twist boundary structures in strontium titanate. *J. Phys. Cond. Matter* **14**, 13635-13641.

BACON, R. (1960): Growth, structure, and properties of graphite whiskers. *J. Appl. Phys.* **31**, 283-290.

CHUKHROV, F.V., ERMILOVA, L.P. & NOSIK, L.P. (1984): On the isotopic composition of carbon in epigenetic graphites. *In* Syngenesis and Epigenesis in the Formation of Mineral Deposits. (A. Wauschkuhn, C. Kluth, R.A. Zimmermann & G.C. Amstutz, eds.) Springer-Verlag, Berlin, Germany (130-137).

DONG, J., SHEN, W., KANG, F. & TATARCHUK, B. (2002): Whiskers with apex angle 135° growing by a disclination growth mechanism. *J. Crystal Growth* **245**, 77-83.

DOUBLE, D.D. & HELLAWELL, A. (1974): Cone-helix growth forms of graphite. *Acta Metall.* **22**, 481-487.

DRESSELHAUS, M.S., DRESSELHAUS, G., AND AVOURIS, P., eds. (2001): *Carbon Nanotubes: Synthesis, Structure, Properties, and Applications.* Springer, New York, N.Y.

DUKE, E.F., & RUMBLE III, D. (1986): Textural and isotopic variations in graphite from plutonic rocks, South-Central New Hampshire. *Contrib. Miner. Petrol.* **93**, 409-419.
EKŞIOĞLU, B. & NADARAJAH, A. (2006): Structural analysis of conical carbon nanofibers. *Carbon* **44**, 360-373.
ENDO, M., KIM, Y.A., HAYASHI, T., FUKAI, Y., OSHIDA, K., TERRONES, M., YANAGISAWA, T., HIGAKI, S. & DRESSELHAUS, M.S. (2002): Structural characterization of cup-stacked-type nanofibers with an entirely hollow core. *Appl. Phys. Lett.* **80**, 1267-1269.
FRANKLIN, R. (1951): The structure of graphitic carbons. *Acta Cryst.* **4**, 253-261.
GALAKHOV, A.V. (1975): *Petrology of the Khibiny alkaline massif*. Nauka, Leningrad, Russia (in Russian).
GILLOT, J., BOLLMANN, W. & LUX, B. (1968) Cristaux de graphite en forme de cigare et a structure conique. *Carbon* **6**, 381-387.
GOGOTSI, Y., LIBERA, J.A., KALASHNIKOV, N. & YOSHIMURA, M. (2000): Graphite polyhedral crystals. *Science* **290**, 317-320.
HAANSTRA, H.B., KNIPPENBERG, W.F. & VERSPUI, G. (1972): Columnar Growth of Carbon. *J. Cryst. Growth* **16**, 71-79.
HARRIS, P.J.F. (1999): *Carbon Nanotubes and Related Structures: New Materials for the Twenty-First Century*. Cambridge University Press, Cambridge, United Kingdom.
IIJIMA. S. (1991): Helical microtubules of graphitic carbon. *Nature (London)* **354**, 56-58.
_____, YUDASAKA, M., YAMADA, R., BANDOW, S., SUENAGA, K., KOKAI, F. & TAKAHASHI, K. (1999): Nano-aggregates of single-walled graphitic carbon nano-horns. *Chem. Phys. Lett.* **309**, 165-170.
JASZCZAK, J.A. (1995): Graphite: Flat, fibrous and spherical. *In* Mesomolecules: From Molecules to Materials (G.D. Mendenhall, A. Greenberg, J.F. Liebman, eds.) Chapman & Hall. New York, N.Y. (161-180).
_____ (1997): Unusual graphite crystals from the Lime Crest quarry, Sparta, New Jersey. *Rocks and Minerals* **72**, 330-334.
_____ (2001): Palache's "Contributions to the mineralogy of Sterling Hill, New Jersey": The 900-foot level revisited. *Picking Table* **42**, 6-15.
_____ & ROBINSON, G.W. (2000): Spherical and triskelial graphite from Gooderham, Ontario, Canada. *Rocks and Minerals* **75**, 172-3.
_____, _____, DIMOVSKI, S. & GOGOTSI, Y. (2003): Naturally occurring graphite cones. *Carbon* **41**, 2085-2092.
KOGARKO, L.N., KRAMM, U., BLAXLAND, A., GRAUERT, B. & PETROVA, E. N. (1981): [Age and origin of the alkaline rocks of Khibiny (rubidium and strontium isotopy).] *Dokl. Akad. Nauk SSSR* **260**(4), 1001-1004 (in Russian).
KOSTYLEVA-LABUNTSOVA, E.E., BORUTSKIY, B.E., SOKOLOVA, M.N., SHLYUKOVA, Z.V., DORFMAN, M.D., DUDKIN, O.B. & KOZYREVA, L.V. (1978): *Mineralogy of the Khibiny Massif. Minerals. Vol. 2*. Nauka, Moscow, Russia (in Russian).
KRAMM, U. & KOGARKO, L.N. (1994): Nd and Sr isotope signatures of the Khibina and Lovozero centres, Kola Alkaline Province, Russia. *Lithos **32***, 225-242.
KRISHNAN, A., DUJARDIN, E., TREACY, M.M.J., HUGDAHL, J., LYNUM, S. & EBBESEN, T.W. (1997): Graphitic cones and the nucleation of curved carbon surfaces. *Nature (London)* **388**, 451-454.
KVASNITSA, V.G., YATSENKO, V.N. & ZAGNITKO, V.M. (1998): [Varieties of Graphite Spherulites from deposits and ore occurrences of Ukraine.] *Mineralogicheskii Zhurnal* **20**(2), 34-39. (In Ukrainian with English summary).
LIBERA, J.A. & GOGOTSI, Y. (2001): Hydrothermal Synthesis of Graphite Tubes Using Ni Catalyst. *Carbon* **39**, 1307-1318.
LUQUE, F.J., PASTERIS, J.D., WOPENKA, B., RODAS, M. & BARRENCHEA, J.F. (1998): Natural fluid-deposited graphite: Mineralogical characteristics and mechanisms of formation. *Am. J. Sci.* **298**, 471-498.
MÖSCHEL, C., REICH, A., ASSENMACHER, W., LOA, I. & JANSEN, M. (2001): Onion-like marbles and bats: New morphological forms of carbon. *Chem. Phys. Lett.* **335**, 9-16.
NEMANICH, R. J. & SOLIN, S. A. (1979): First- and second order Raman scattering from finite-size crysals of graphite. *Phys. Rev. B* **20**, 392-401.
OBERLIN, A., ENDO, M. & KOYAMA, T. (1976): Filamentous growth of carbon through benzene decomposition. *J. Crystal Growth* **32**, 335-349.
PALACHE, C. (1941): Contributions to the mineralogy of Sterling Hill, New Jersey: Morphology of graphite, arsenopyrite, pyrite and arsenic. *Am. Mineral*. **26**, 709-717.
PATEL, A.R. & DESHAPANDE, S.V. (1970): Whisker growth in natural graphite. *Carbon* **8**, 242.
PASTERIS, J.D. (1999): Causes of the uniformly high crystallinity of graphite in large epigenetic deposits. *J. Metamorphic Geol.* **17**, 779-787.
PHILLPOT, S., WOLF, D., & LUTSKO, J.F. (1990): Anomalous elastic behavior in superlattices of twist grain boundaries in silicon. *J. Appl. Phys.* **67**, 6747-6759.

RUMBLE III, D., DUKE, E.F. & HOERING, T.L. (1986): Hydrothermal graphite in New Hampshire: Evidence of carbon mobility during regional metamorphism. *Geology* **14**, 452-455.
_____ & HOERING, T.L. (1986): Carbon isotope geochemistry of graphite vein deposits from New Hampshire, U.S.A. *Geochim. Cosmochim. Acta* **50**, 1239-1247.
SAITO, Y., YOSHIKAWA, T., BANDOW, S., TOMITA, M. & HAYASHI, T. (1993): Interlayer spacings in carbon nanotubes. *Phys. Rev. B* **48**, 1907-1909.
SPECK, J.S., ENDO, M. & DRESSELHAUS, M.S. (1989): Structure and intercalation of thin benzene derived carbon fibers. *J. Crystal Growth* **94**, 834-848.
TAN, P.H., DIMOVSKI, S. & GOGOTSI, Y. (2004): Raman scattering of non-planar graphite: arched edges, polyhedral crystals; whiskers and cones. *Phil. Trans. Royal Soc. London A* **362**, 2289-2310.
TERRONES, H., HAYASHI, T., MUÑOZ-NAVIA, M., TERRONES, M., KIM, Y.A., GROBERT, N., KAMALAKARAN, R., DORANTES-DÁVILA, J., ESCUDERO, R., DRESSELHAUS, M.S. & ENDO, M. (2001): Graphitic cones in palladium catalyzed carbon nanofibers. *Chem. Phys. Lett*. **343**, 241-250.
THOMSEN, C. & REICH, S. (2000): Double Resonant Raman Scattering in Graphite. *Phys. Rev. Lett.* **85**, 5214-5217.
UGARTE, D. (1995): Onion-like graphitic particles. *Carbon* **33**, 989-993.
WEIS, P. (1980): Graphite skeleton crystals- A newly recognized morphology of crystalline carbon. *Geology* **8**, 296-297.
WOLF, D. (1984): Properties of high-angle (001) twist grain boundaries in alkali-halide bicrystals: A theoretical investigation. *Phil. Mag.* A **49**, 823-844.
_____ (1989): Structure-energy correlation for grain boundaries in f.c.c metals- I. Boundaries on the (111) and (100) planes. *Acta Metall.* **37**, 1983-1993.
_____ (1990): Structure-energy correlation for grain boundaries in f.c.c. metals- IV. Asymmetrical twist (general) boundaries. *Acta Metall.* **38**, 791-798.
YAKOVENCHUK, V.N., IVANIUK G.Yu., PAKHOMOVSKIY, Ya.A. & MEN'SHIKOV Yu.P. (1999): *Minerals of the Khibiny massif*. Zemlya, Moscow, Russia (in Russian).
_____, _____, _____ & _____ (2005): *Khibiny*. (F. Wall, ed.) Lapplandia Minerals, Apatity, Russia.
ZAK, S.I., KAMENEV, E.A., MINAKOV, F.V., ARMAND, A.L., MIKHEICHEV, A.S. & PETERSIL'YE I.A. (1972): *The Khibiny Alkaline Massif.* Nedra, Leningrad, Russia (in Russian).
ZHANG. G., JIANG, X. & WANG, E. (2003) Tubular graphite cones. *Science* **300**, 472-474.

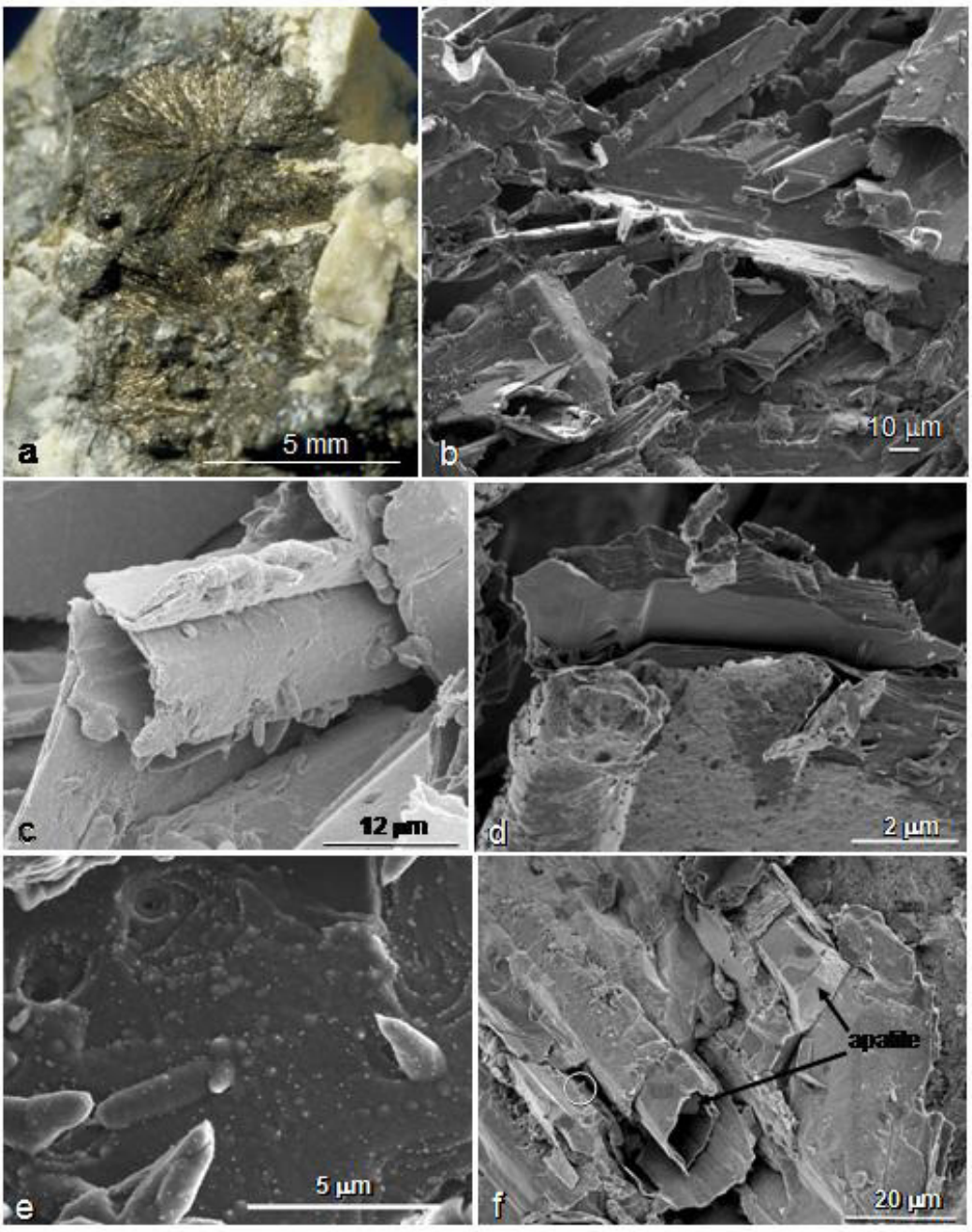


**Figure 1**

FIG. 1. (a) Optical photograph of a 7-mm spherical cluster of radially-aligned graphite fibers with K-feldspar, strontian fluorapatite and aegirine. (b-d) FESEM images of hollow graphite fiber channels and associated RGS. (c) Higher magnification image of RGS on a hollow graphite channel. What appears to be a crushed graphite channel rests above an open, empty channel. (d) Close up of a broken channel wall showing the graphite lamellae and the secondary graphite overgrowth. (e) Close-up of RGS growing out of the secondary graphite overgrowth. Note the circular depressions at the upper left where RGS have broken away. (f) Strontian fluorapatite crystals inside graphite channels. A conical rolled graphitic structure is circled at the left.

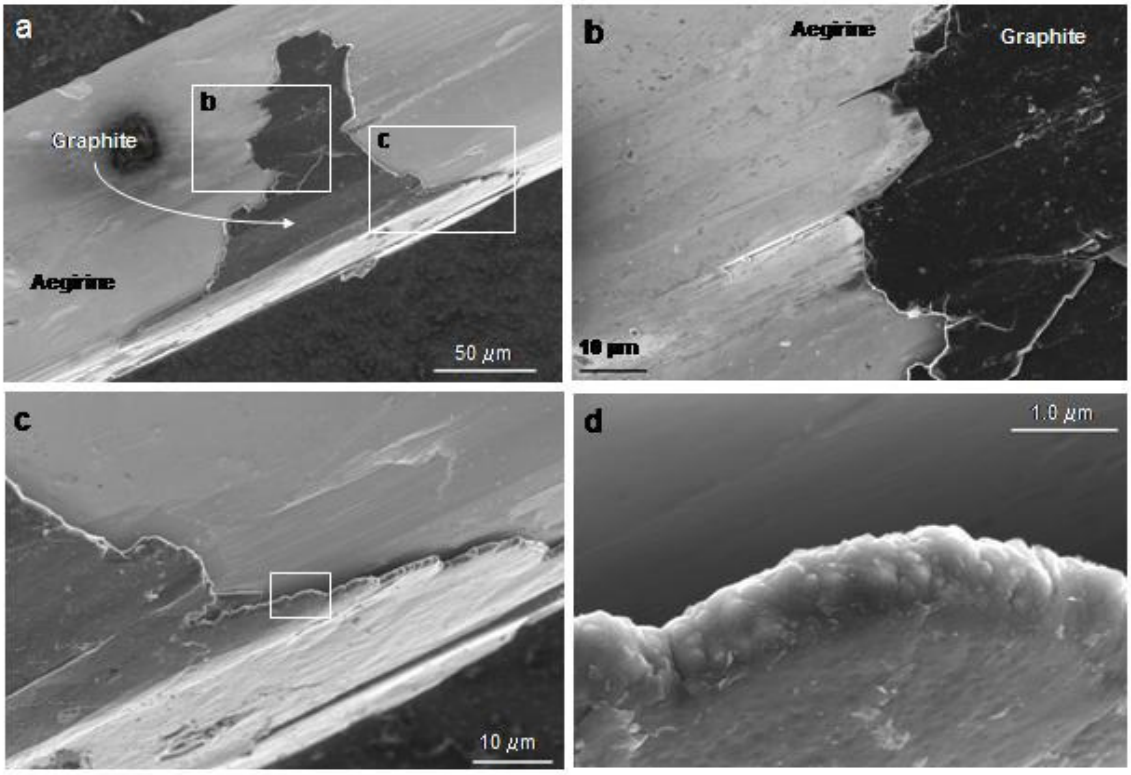


**Fig. 2**

FIG. 2. FESEM images of graphite overgrown on and partially intergrown with aegirine. Higher magnification images of selected regions in (a) are shown in respective images (b) and (c). Region (b) shows aegirine partially grown on top of graphite (top center) as well as graphite grown on top of the aegirine (bottom center). Region (c) shows the edge of the thin graphite overgrowth. (d) higher magnification image of the graphite edge in (c) showing the fine-scale texture of the graphite overgrowth.

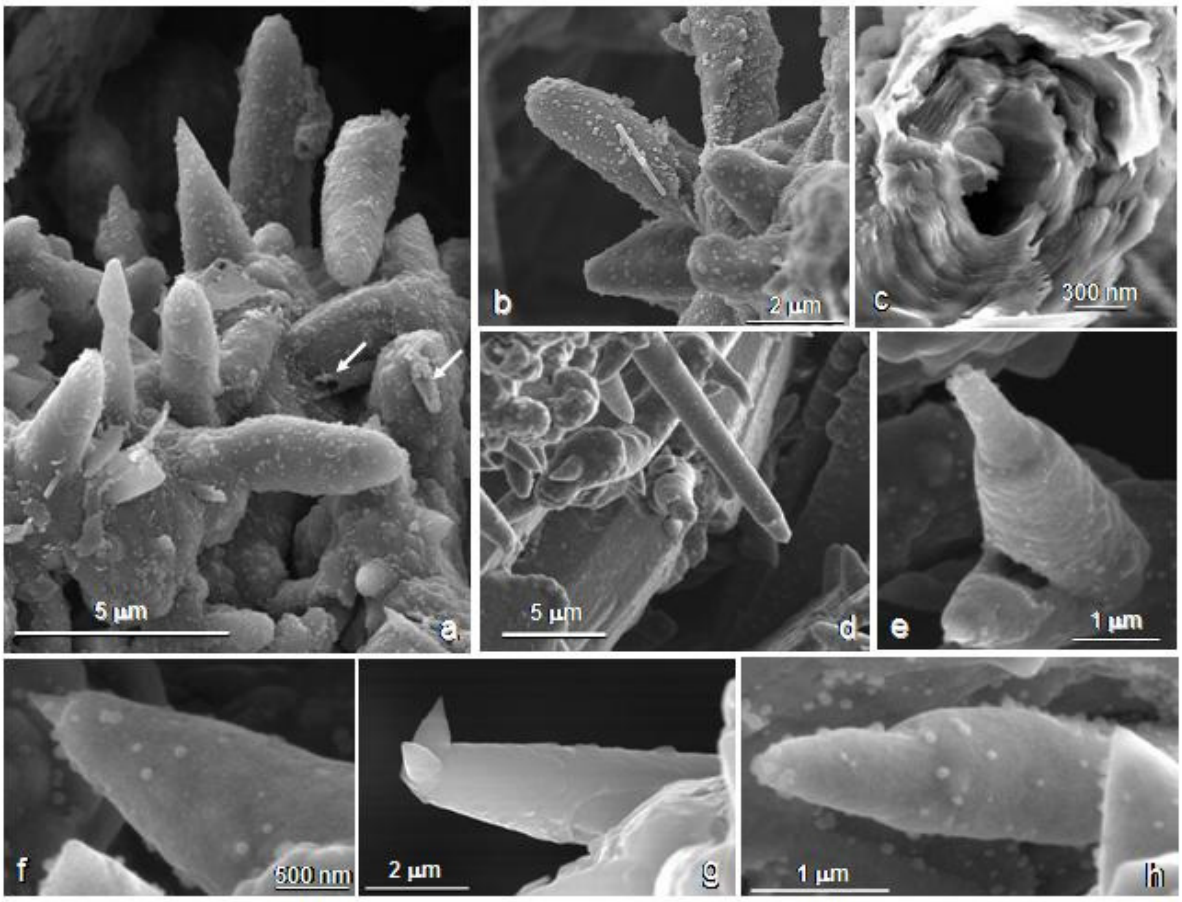


**Fig. 3**

FIG. 3. (a-h) FESEM images of RGS of varying morphologies, coating the surfaces of aegirine and associated minerals in fractures in the pegmatite. Arrows in (a) indicate a few of the hollow broken tubes and cones. (b) Blunt-tipped RGS associated with a large nano-scale tube. (c) Broken scroll revealing a hollow center with concentric graphite layered walls. (d-h) Scrolls and cones showing a variety of morphologies.

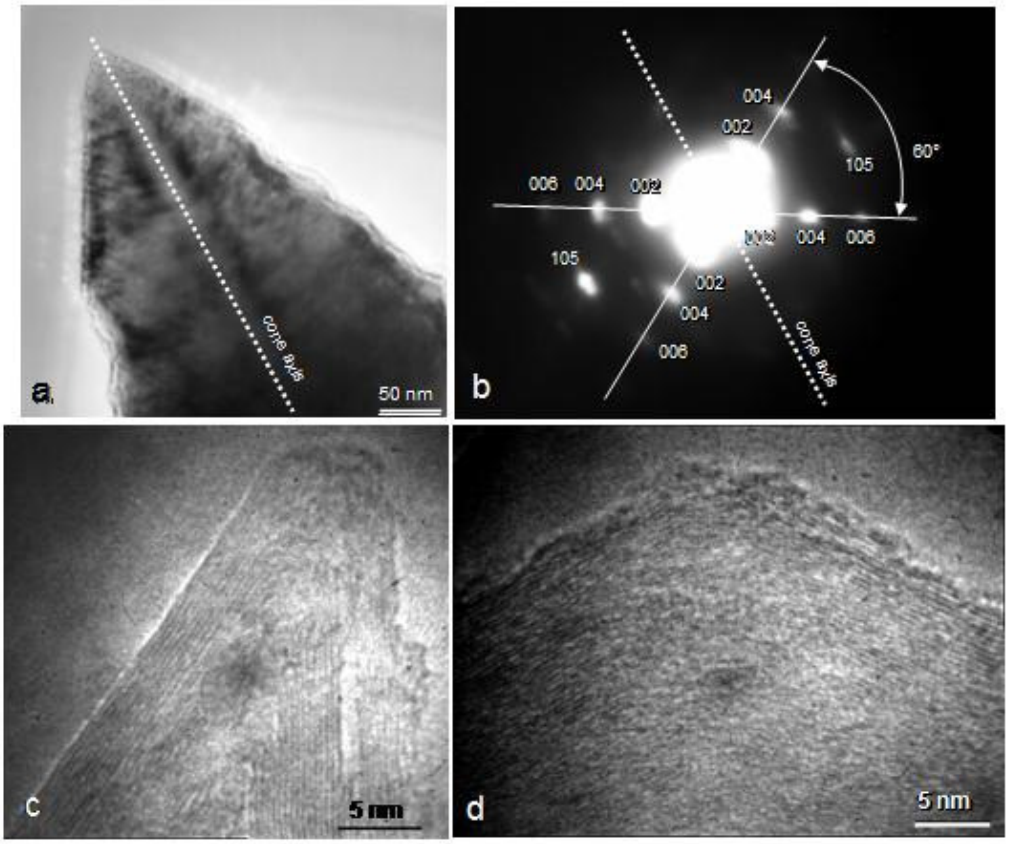


**Fig. 4**

FIG. 4. (a) TEM image of a graphite cone with a 60° apex angle and (b) associated electron diffraction pattern from the center of the cone indicating that the graphene sheets are aligned parallel to the conical surface. The surface of the cone is coated by an amorphous carbon layer several nanometers thick. (c) HRTEM image of a graphite nanocone with ~39°-apex angle showing well-ordered lattice fringes parallel to the cone surface. (d) HRTEM image of a graphite nanocone with a ~126° apex angle showing disordered lattice fringes.

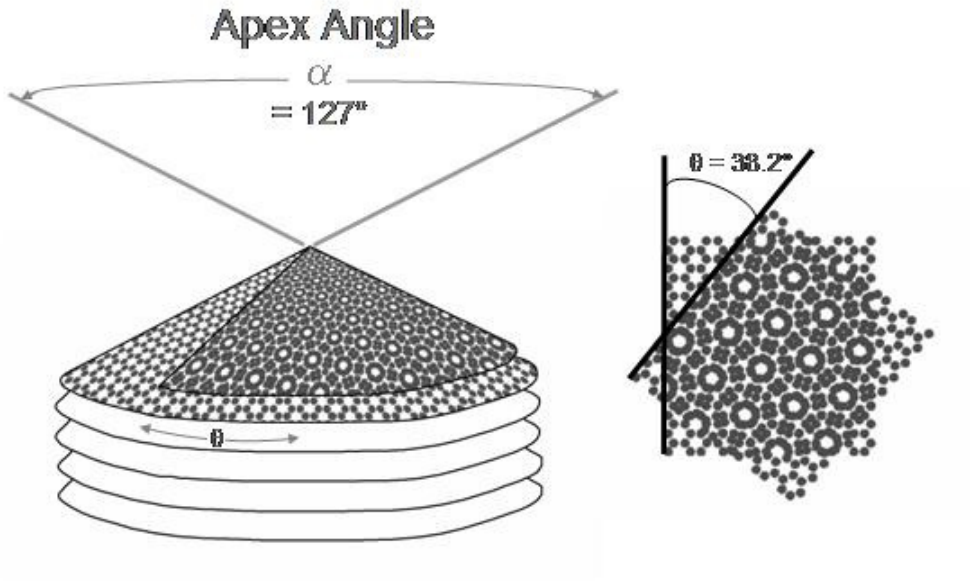


Fig. 5

FIG. 5. Schematic of the cone-helix model (modified after Double and Hellawell 1974) for a cone with an apex angle $\alpha = 127°$ resulting from an overlap angle $\theta = 60° - 21.8° = 38.2°$ illustrating a moiré pattern from the lattice coincidences between adjacent graphene layers.

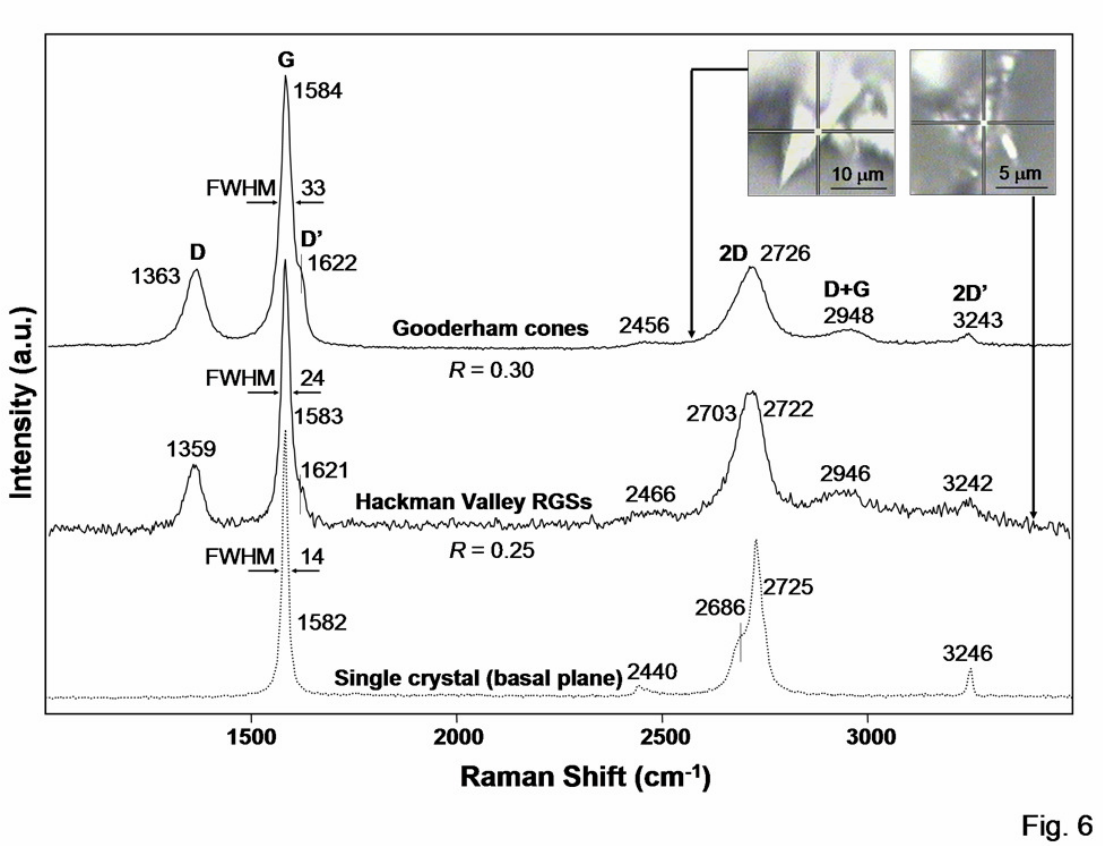


Fig. 6

FIG. 6. Comparison of Raman spectra, after baseline correction, from single crystal graphite, naturally occurring graphite cones from Gooderham, Ontario, and micron-sized RGS from Hackman Valley, Kola Peninsula, Russia. Cross-hairs in the optical images of the insets indicate the positions of the Raman probe for the respective spectra. FWHM denotes the full width at half maximum for each corresponding G peak. *R* values correspond to the D/G line intensity ratios for the Gooderham cones and the Hackman Valley RGS.